Three-dimensional-printed titanium prostheses with bone trabeculae enable mechanical-biological reconstruction after resection of bone tumours

Feifei Pu#, Wei Wu#, Doudou Jing#, Yihan Yu, Yizhong Peng, Jianxiang Liu, Qiang Wu, Baichuan Wang, Zhicai Zhang*, Zengwu Shao*

Key Words:
bone defect; bone tumour; printed biomechanical reconstruction; prostheses; three-dimensional

From the Contents

ABSTRACT

Reconstruction after resection has always been an urgent problem in the treatment of bone tumours. There are many methods that can be used to reconstruct bone defects; however, there are also many complications, and it is difficult to develop a safe and effective reconstruction plan for the treatment of bone tumours. With the rapid development of digital orthopaedics, three-dimensional printing technology can solve this problem. The three-dimensional printing of personalised prostheses has many advantages. It can be used to print complex structures that are difficult to fabricate using traditional processes and overcome the problems of stress shielding and low biological activity of conventional prostheses. In this study, 12 patients with bone tumours were selected as research subjects, and based on individualised reverse-engineering design technology, a three-dimensional model of each prosthesis was designed and installed using medical image data. Ti6Al4V was used as the raw material to prepare the prostheses, which were used to repair bone defects after surgical resection. The operation time was 266.43 ± 21.08 minutes (range 180–390 minutes), and intraoperative blood loss was 857.26 ± 84.28 mL (range 800–2500 mL). One patient had delayed wound healing after surgery, but all patients survived without local tumour recurrence, and no tumour metastasis was found. No aseptic loosening or structural fracture of the prosthesis, and no non-mechanical prosthesis failure caused by infection, tumour recurrence, or progression was observed. The Musculo-Skeletal Tumour Society (MSTS) score of limb function was 22.53 ± 2.09 (range 16–26), and ten of the 12 patients scored ≥ 20 and were able to function normally. The results showed that three-dimensional printed prostheses with an individualised design can achieve satisfactory short-term clinical efficacy in the reconstruction of large bone defects after bone tumour resection.

Introduction

Malignant bone tumours are a serious hazard to human health, and are the third leading cause of death among cancer patients younger than 20 years old.[1] At present, the treatment of bone tumours is mainly chemotherapy combined with surgical resection. Because patients with bone tumours are often children and adolescents, they have high requirements for the recovery of limb function after surgery; however, to prevent local recurrence during surgical resection, the resection scope is often enlarged.[2] Therefore, reconstruction after resection is an urgent problem to be solved in the treatment of bone tumours. There are many methods of reconstruction, which can be roughly divided into biological reconstruction, mechanical reconstruction, and allograft reconstruction.[3] However, complications such as fractures, non-union, delayed union, or infection still occur in all of these reconstruction programs, forcing patients to undergo multiple revision surgeries and even amputation.[4] Consequently, it is difficult to develop a safe and effective reconstruction plan for bone tumour treatment.

The modular prosthesis is a common clinical method for the reconstruction of limb bone defects, but the product has a poor fit with

patients, and the attachment points of ligaments and other soft tissues are difficult to match, resulting in poor accuracy. Because of the special function of the limb bone, a modular prosthesis may not meet the requirements of load bearing and stability.[5] With the rapid development of digital orthopaedics, three-dimensional (3D) printing technology can solve this problem. With the help of digital imaging data and digital geometric anatomy, personalised prostheses with the same shape as the patient's diseased tissue are 3D-printed.[6] Such 3D-printed personalised prostheses have many outstanding advantages, including accuracy, stability, economy, and speed. This method can be used to print complex structures that are difficult to fabricate by traditional processes, and the problems of stress shielding and low biological activity of conventional prostheses have been overcome.[7]

In recent years, the broad application of titanium alloy materials has proved that these materials have good mechanical properties and biocompatibility.[8] After titanium alloy prosthesis implantation, the surface can be oxidised to form a dense TiO film, which further reduces the body's rejection reaction to the material and increases bone integration. Titanium alloy materials exhibit excellent mechanical properties, low density, and good fatigue performance. Compared with other medical metal materials (stainless steel, etc.), their elastic modulus is lower and closer to the elastic modulus of human cortical bone, which can significantly reduce stress shielding and stress concentration.[9] The pore structure of this porous material is also more conducive to bone repair and reconstruction. Porous titanium alloy materials have good mechanical properties that can promote the adhesion and proliferation of osteoblasts. Moreover, an appropriate pore structure can promote bone ingrowth. The bond between the bone and porous titanium alloy has been proven to be superior to that of solid titanium alloy.[10]

As no unified standard has yet been developed for the design and preparation methods of 3D-printed prostheses, the best way to more scientifically and accurately reconstruct a defect after resection of a bone tumour remains to be further discussed. In this study, patients with bone tumours were selected as the research subjects, and based on individualised reverse-engineering design technology, a three-dimensional model of the prosthesis was designed and installed using medical image data. Ti6Al4V was used as the raw material to prepare the prosthesis and was applied to the repair of bone defects after surgical resection. Postoperative follow-up was conducted for imaging evaluation and evaluation of the clinical efficacy.

Methods
Ethics statement
This study was approved by the Ethics Committee of Union Hospital, Tongji Medical College, Huazhong University of Science and Technology (approval No. 2019-IEC-S274) in 2019, and all patients provided signed informed consent forms.

Three-dimensional reconstruction of tumour invasion area
Preoperative X-ray, thin computed tomography (CT) scan, magnetic resonance imaging (MRI), and single-photon emission computed tomography/CT were performed at the operative site in each patient, and CT scan data were recorded in Dicom format on CD. The CT scan data were imported into the medical image segmentation processing software Mimics 19.0 (Materialise, Leuven, Belgium). First, the pixel to be obtained was selected by adjusting the threshold value, and then manual operation of the draw and erase functions was performed to select the image. The 3D reconstruction data of the tumour sites were obtained using a 3D operation (**Figure 1A** and **B**).

Figure 1. Image data acquisition and 3D reconstruction of tumour invasion area. (A, B) The CT scan data were imported into the medical image segmentation processing software Mimics 19.0 for image selection processing. The red arrows indicate the tumour. (C) The 3D operation to create the 3D reconstruction data of the tumour site. The blue indicates normal bone, the red indicates the bone invaded by the tumour, and the boundary between blue and purple represent the osteotomy line. B: below; L: left; T: top.

*Corresponding authors:
Zengwu Shao, 1985XH0536@hust.edu.cn; Zhicai Zhang, zhicaizhang@hust.edu.cn.

#Author Equally.

Department of Orthopaedics, Union Hospital, Tongji Medical College, Huazhong University of Science and Technology, Wuhan, Hubei Province, China

Determination of osteotomy plane for tumour resection

According to the principle of tumour resection, the location of the resection site in relation to a certain anatomical marker was measured by referring to the location of the tumour boundary examined by MRI to provide an accurate size. The resection boundary, osteotomy plane, and angle were measured and determined using Mimics 19.0 software. The resection scope of malignant tumours is mainly based on osteotomy of normal bone 2–3 cm outside the tumour boundary, as shown by MRI examination or CT scan (**Figure 1C**).

3D printing of customised prosthesis design

The bone defect model obtained from Mimics 19.0 was imported into the reverse-engineering software Geomagic Studio 12 (Geomagic, Rock Hill, NC, USA) for modification, which smoothly connected the designed steel plate to the bone defect prosthesis and added a beam-column structure for mechanical strength to obtain a blank prosthesis (**Figure 2A** and **B**). Subsequently, the solid and porous parts were segmented using the STL file-editing software Magics 21.0 (Magics, Materialise), and the porous unit was selected. According to the shape and structure of different prostheses, the characteristics of various software functions were adjusted repeatedly to obtain a complete prosthesis (**Figure 2C–G**).

Computer simulation of cutting and installation

Mimics 19.0 software was used to simulate the model cutting and installation of the prosthesis, then the cutting and installation were carried out in accordance with the plan. The size, degree of fitting, and screw position of the prosthesis were further evaluated according to the degree of matching (**Figure 3A–C**). For any design that did not meet surgical requirements, redesign or local modification and optimisation were needed. The size error of fitting in all directions to the prosthesis model was less than 0.5 mm, the direction of the screw channel overlapped with the planned channel and the direction of the screw implantation was not blocked by important neurovascular tissue.

Preparation of 3D-printed personalised metal prostheses and navigation templates

In accordance with the model, the Ti alloy (Ti6Al4V) was quickly printed by selective laser melting, and the parts were polished, processed, cleaned, and sterilised before use (**Figure 4A** and **B**). To ensure the precision of prosthesis implantation, a navigation template was designed according to differences in the patients' anatomical structures and surgical needs (**Figure 5A–C**). Through navigation verification, tracking, and monitoring during surgery, precise resection of the tumour and fine reconstruction of the customised prosthesis were performed.

Operation method

During the operation, an incision was created according to the established plan, the bone surface was exposed, osteotomy was guided by the navigation template, and the tumour was removed (**Figure 6A–C**). The prosthesis was then placed in the defect and secured with screws (**Figure 6D–F**). Intraoperative negative pressure drainage was performed, and a postoperative negative pressure drainage tube was placed for 1 week. An inflatable lower-extremity pump was used to prevent lower-extremity deep vein thrombosis. Antibacterial treatment was administered for 3 days, and the stitches were removed after wound healing.
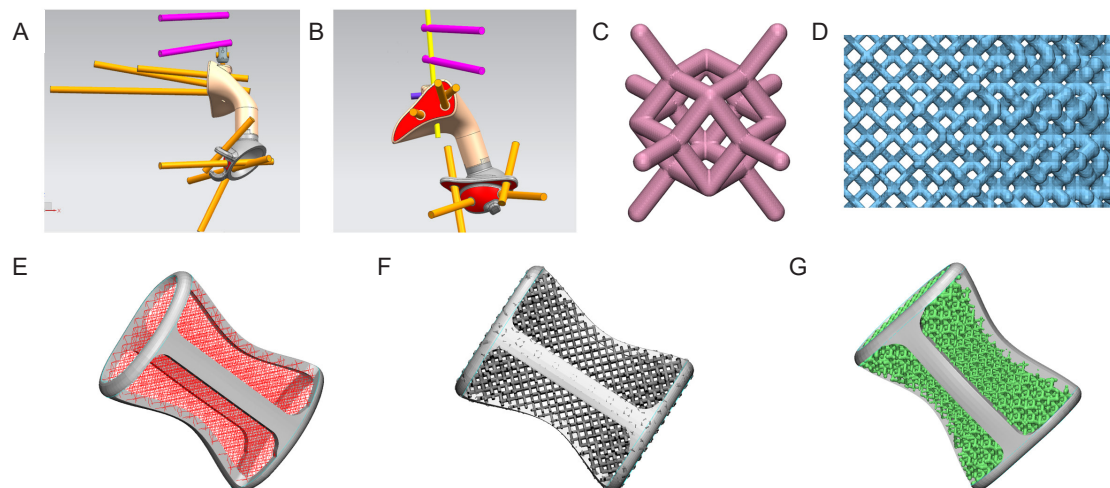

Figure 2. Design of three-dimensional printed customised prostheses. (A, B) Designing the size, fit and screw position of the prosthesis in different viewing angles. The pink and yellow sticks represent screws and connecting rods. (C) The dodecahedral lightweight lattice structure. (D) The gradient mesh designed according to the stress distribution identified by finite element analysis. (E) Design of prosthetic stiffeners and dodecahedron grid array diagram. (F) Design of gradient grid. (G) Physical design of the prosthesis.
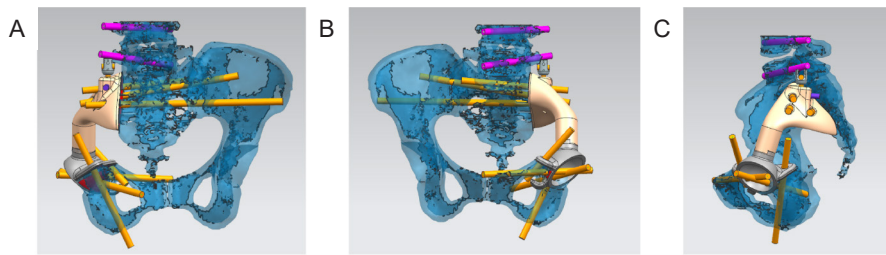
Figure 3. Computer simulation cutting and installation. (A–C) Mimics 19.0 software was used to simulate model cutting and prosthetic installation in different viewing angles.
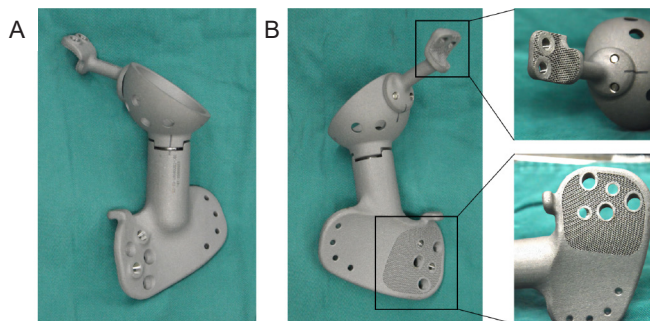

Figure 4. Preparation of three-dimensional printed personalised titanium alloy prostheses. (A, B) Titanium alloy (Ti6Al4V) was used for rapid printing by selective laser melting, and the surface interface of the prosthesis was created with a porous bone trabecular structure.
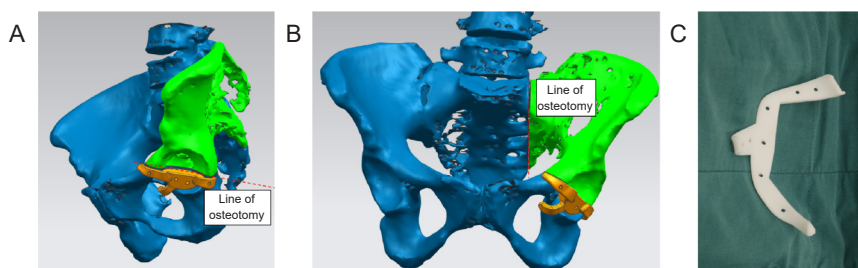

Figure 5. Three-dimensional printed navigation template design and processing. (A, B) The navigation template was designed according to the patient's anatomical structure and surgical needs in different viewing angles. The green colour shows the part needing to be removed. (C) Preparation of the navigation template to assist with precise tumour resection.
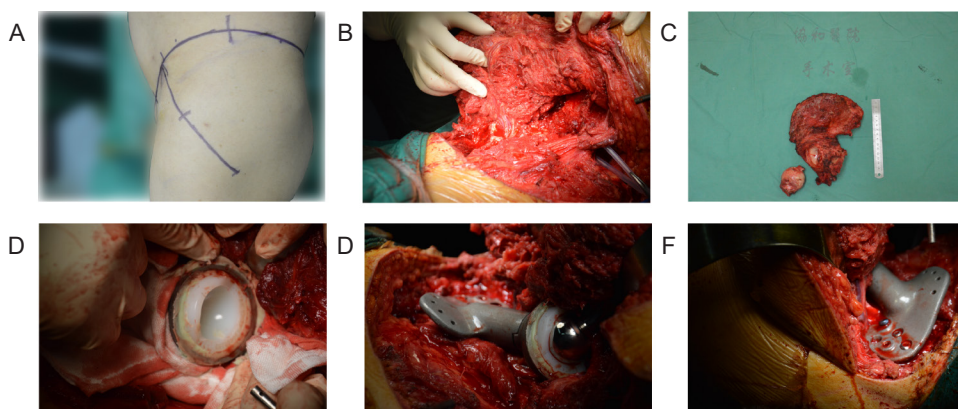

Figure 6. Implantation of a three-dimensional printed prosthesis to reconstruct a bone defect after tumour resection. (A) Surgical position and incision. (B) *En bloc* resection of the tumour. (C) Gross view of the excised tumour specimen. (D) Installation of the acetabular prosthesis. (E) Placing of the three-dimensional printed prosthesis in the defect. (F) The three-dimensional printed prosthesis was secured with screws.

Postoperative treatment

After the operation, antibiotic treatment was administered, and an inflatable leg pump was used to prevent venous thrombosis of the lower limbs. The drainage tube was removed when the daily drainage volume was less than 50 mL. After the drainage tube was removed, the patient was encouraged to walk and undergo rehabilitative training. After surgery, chemotherapy, radiotherapy and molecular-targeted therapy were used to treat the primary tumour.

Follow-up and evaluation indicators

The follow-up mainly involved evaluation of the patient's signs, symptoms, and imaging findings. The efficacy evaluation mainly comprised survival, disease, complications, and limb function. Evaluation of lower limb function based on the MSTS score was performed 3 months after surgery.[11] The MSTS score consists of seven items: pain, mobility, strength, joint stability, deformity, emotional acceptance, and overall function. The score of each item is from 0 to 5 points, and the maximum total score is 35 points. A higher score indicates better function.

Statistical analysis

The patient's pain level and limb function were analysed using SPSS 20.0 (IBM, Armonk, NY, USA). The Chi-square test was used to compare the classification variables between the groups. Independent sample *t*-tests were used for intergroup comparisons of continuous variables, and paired *t*-tests were used to compare the MSTS scores. Statistical significance was set at $P < 0.05$.

Results

General results

Personalised 3D-printed titanium alloy prostheses were successfully designed and prepared, and tumour resection and 3D-printed prosthetic weight construction surgery were completed in all 12 patients according to the preoperative

design (**Table 1**). The operation time was 266.43 ± 21.08 minutes (range 180–390 minutes), and intraoperative blood loss was 857.26 ± 84.28 mL (range 800–2500 mL).

No adverse reactions occurred during the surgery. One patient experienced delayed wound healing after surgery, while the rest recovered well with no instances of fever, infection, or other related complications.

Oncology results

All patients were effectively followed up for 7–24 months, with an average follow-up time of 15.59 ± 6.21 months. Up to the last follow-up, all patients had survived without local tumour recurrence, and no tumour metastasis was found at any postoperative follow-up.

Imaging evaluation

All patients underwent tumour osteotomy according to the preoperative design and osteotomy guide plate, the prosthesis was installed stably, and the bone ends showed good anastomosis with both ends of the prosthesis. At each follow-up, no aseptic loosening or structural fractures of the prosthesis were observed in any of the 12 patients, and no non-mechanical prosthesis failure caused by infection, tumour recurrence, or progression was observed (**Figure 7A–F**).

All patients underwent radiographic examination after surgery, which showed that the 3D-printed prostheses implanted in all patients were consistent with the shape and size of the osteotomy surface, and the match was accurate. The position, length, and direction of the screws in all the patients were consistent with the preoperative design.

MSTS function score

By the last follow-up, all 12 patients were able to carry out full weight bearing, and the MSTS score of lower limb function was 22.53 ± 2.09 (range 16–26). Ten scored ≥ 20 and were able to function normally.

Table 1. Commonly-used gene- and cell-activated biomaterials

No.	Sex	Age (years)	Pathological type	GTV (cm³)	FU (months)	SD (minutes)	IBL (mL)	PC	TR	DM	MSTS score
1	Male	42	Ewing's sarcoma	320	16	375	1800	No	No	No	22
2	Female	37	Malignant neurinoma	360	14	260	2500	No	No	No	25
3	Female	58	Osteosarcoma	460	12	265	800	No	No	No	18
4	Male	69	Chondrosarcoma	300	23	270	2500	No	No	No	20
5	Male	58	Chondrosarcoma	350	7	180	2000	Skin necrosis	No	No	23
6	Male	42	Osteosarcoma	290	24	245	1800	No	No	No	20
7	Male	63	Invasive GCTB	340	14	255	2500	No	No	No	21
8	Male	50	Osteosarcoma	260	18	375	2000	No	No	No	24
9	Male	53	Osteosarcoma	280	16	280	2200	No	No	No	26
10	Female	48	Chondrosarcoma	300	12	320	1500	No	No	No	16
11	Male	53	Chondrosarcoma	260	18	260	2200	No	No	No	24
12	Female	46	Chondrosarcoma	280	22	235	2300	No	No	No	20

Note: DM: distant metastasis; FU: follow-up; GCTB: giant cell tumour of bone; GTV: gross tumour volume; IBL: intraoperative blood loss; MSTS: Musculo-Skeletal Tumour Society; PC: postoperative complication; SD: surgical duration; TR: tumour recurrence.
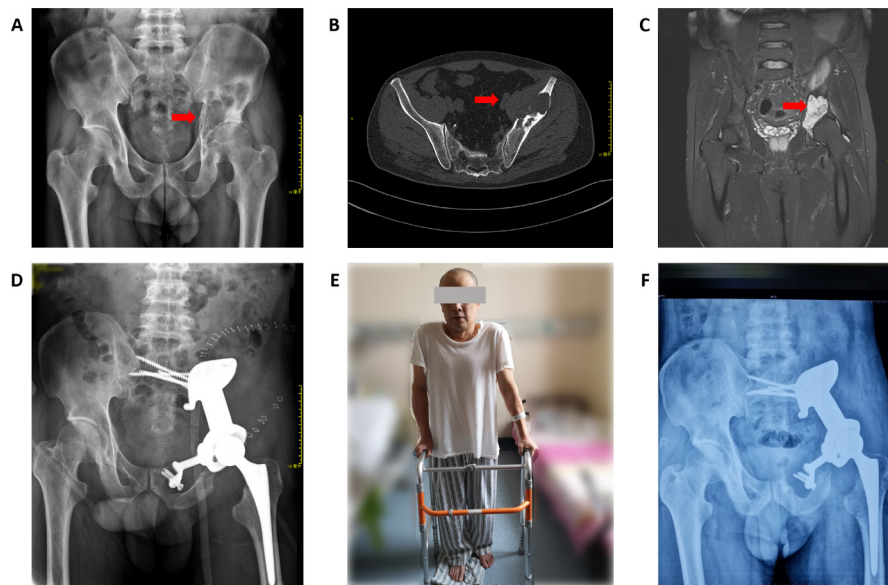
Figure 7. A 53-year-old patient with chondrosarcoma of the pelvis underwent reconstruction with a three-dimensional-printed prosthesis to repair the bone defect after tumour resection. (A–C) Preoperative X-ray images (A), computed tomography (B), and magnetic resonance imaging (C). The red arrows indicate the tumour. (D) One week postoperatively, X-ray imaging showed good position and stability of the prosthesis. (E) One week postoperatively, the patient was walking with the aid of a walker. (F) Six months after the operation, X-ray imaging showed good fusion of the prosthesis with the bone, without fracture or other complications.

Discussion

Due to the significant difference between bone density and density of the surrounding tissue, the difference in grey values presented by CT and MRI systems and the surrounding tissue can be detected by computer and recognised by the naked eye, making it is easier to distinguish and reconstruct using imaging software.[12] Due to the special role of bone in the human body and its physical characteristics, 3D-printed prostheses have many advantages for the treatments of bone defects and are more and more widely used.[13] Current applications mainly include 3D-printed models, navigation templates and personalised prostheses, and satisfactory results have been achieved by the application of these technologies in the field of orthopaedics.[14] For bone defect prostheses, a variety of products have been approved for clinical use.

A 3D-printed navigation template is an instrument that can be accurately matched and guided during surgery. The application of navigation templates in pedicle screw implantation guidance has reduced the difficulty of the operation for surgeons. Its advantages of simple operation, accurate control, and reduced operation time can reduce the risk of neurovascular injury during surgery and reduce the occurrence of complications.[15] The application of 3D-printed personalised navigation templates in various surgical treatments, such as bone tumour resection and reconstruction, bone tumour lesion biopsy, and fracture prosthesis orientation, has become common.[16, 17]

Titanium alloy materials exhibit good mechanical properties and biocompatibility. The elastic modulus of titanium alloy solid material is 110 GPa, higher than that of normal cortical bone at 15 GPa, resulting in the problem of stress shielding,

increased likelihood of bone resorption and poor integration of the bone with the metal interface.[18] Titanium alloy is an inert material, and the solid surface does not stimulate the growth of adjacent bones, so it cannot promote the amount and speed of bone ingrowth.[19] In order to overcome the above problems, changing the material configuration is a good solution, and porous titanium alloy was born. By controlling key parameters such as porosity and pore size, the apparent elastic modulus of the titanium alloy can be effectively reduced to match the elastic modulus of bone. Tantalum has similar physical and chemical properties to titanium, and studies have shown that tantalum has good biocompatibility and bone integration.[20] However, tantalum metal has a high melting point making 3D printing difficult, and consequently product development is relatively lagging behind. Previous studies have shown that 3D-printed porous tantalum has better bioactivity and bone integration ability than porous titanium or titanium alloy. However, the pore size parameters of porous titanium, porous titanium alloy and porous tantalum are not consistent, and research into bone repair using porous titanium or porous tantalum with the same parameters is limited.[21, 22]

Cancellous bone has a porosity of 50–90%, and consists of a trabecular mesh framework with an aperture of approximately 1.0 mm. Cortical bone has a porosity of 3–12%, and is dense in structure.[23] Metal bone trabeculae are similar to human bone trabeculae, and their elastic modulus is comparable to that of human bone tissue. A porous titanium alloy scaffold with better pore connectivity has the advantage of enabling the elastic modulus of the scaffold to be reduced to approximately 20 GPa by changing the pore diameter and wire diameter,

making it closer to the elastic modulus of bone tissue, thus further reducing the stress shielding effect and promoting bone integration. The widely-distributed porous interconnected structure also facilitates the circulation of nutrients in adjacent tissues, stimulates the growth and proliferation of osteoblasts, and allows the material to bind more firmly and closely with surrounding bone tissues.[24, 25]

There is a theoretical basis for the expected long-term efficacy of implanted 3D-printed personalised prostheses. Compared with other prostheses, 3D-printed personalised prostheses have many advantages: they are fast and convenient to make, can be shaped accurately, and they are stable in the body, with good biological activity and strong mechanical stability.[26] Compared with traditional prostheses, another outstanding feature of 3D-printed personalised prostheses is their accuracy and stability.[27] The personalised prosthesis design enables each patient to be given the unique best implant, which is also the best performance of precision medicine, and is conducive to the recovery of patients' limb function after surgery. From the perspective of 3D-printed prosthesis theory, the technology uses software to generate 3D images, and to perform processes including editing, surface smoothing, model segmentation, etc., to ensure that the accuracy of 3D-printed prostheses is up to standard.[28]

In this study, by the last follow-up, the MSTS score of limb function was 22.53 ± 2.09 (range 16–26). Ten (83%) of the patients scored ≥ 20 and were able to function normally. We analysed the possible reasons for good functionality, and concluded that a precise preoperative approach analysis determined the best approach to minimise muscle injury; complete pelvic ring and in situ acetabular reconstruction ensured 3D stability and normal stress conduction of the pelvis; while during the operation, the bone tissue of the muscle attachment point was preserved as much as possible to enhance stability during the reconstruction of the muscle insertion point. A 3D-printed prosthesis is more suitable for the curved shape of the iliac outer plate, and the screws can be accurately placed into the S1 and/or S2 vertebrae. Additionally, the use of long cancellous bone screws and short cortical screws to fix the prosthesis can achieve more stable fixation and natural mechanical conduction.

This study has some limitations. First, this was a retrospective case-control study, which inevitably was prone to selection bias. Second, the overall postoperative follow-up time was short, which may have led to underestimation of the incidence of mechanical complications such as aseptic loosening and screw fracture. Third, this was a small-sample study in a single centre, and a large study in multiple centres is needed. Finally, the effect of the 3D-printed prosthesis on bone growth needs to be confirmed by a longer follow-up period.

In conclusion, individually-designed 3D-printed prostheses can be used to reconstruct large bone defects after bone tumour resection, and satisfactory short-term clinical efficacy can be obtained. The medium- and long-term efficacy is expected to be good. 3D-printed prostheses with individualised designs have broad application prospects and great development potential.

Conflicts of interest statement

We declare that we have no conflicts of interest.

Editor note: Zengwu Shao is an Editorial Board member of *Biomaterials Translational*. He was blinded from reviewing or making decisions on the manuscript. The article was subject to the journal's standard procedures, with peer review handled independently of this Editorial Board member and his research group.

1. Strauss, S. J.; Whelan, J. S. Current questions in bone sarcomas. *Curr Opin Oncol.* **2018**, *30*, 252-259.

2. Zekry, K. M.; Yamamoto, N.; Hayashi, K.; Takeuchi, A.; Alkhooly, A. Z. A.; Abd-Elfattah, A. S.; Elsaid, A. N. S.; Ahmed, A. R.; Tsuchiya, H. Reconstruction of intercalary bone defect after resection of malignant bone tumor. *J Orthop Surg (Hong Kong).* **2019**, *27*, 2309499019832970.

3. Gangi, A.; Tsoumakidou, G.; Buy, X.; Quoix, E. Quality improvement guidelines for bone tumour management. *Cardiovasc Intervent Radiol.* **2010**, *33*, 706-713.

4. Piccioli, A.; Rossi, B.; Sacchetti, F. M.; Spinelli, M. S.; Di Martino, A. Fractures in bone tumour prosthesis. *Int Orthop.* **2015**, *39*, 1981-1987.

5. Severyns, M.; Briand, S.; Waast, D.; Touchais, S.; Hamel, A.; Gouin, F. Postoperative infections after limb-sparing surgery for primary bone tumors of the pelvis: Incidence, characterization and functional impact. *Surg Oncol.* **2017**, *26*, 171-177.

6. Pu, F.; Liu, J.; Shi, D.; Huang, X.; Zhang, J.; Wang, B.; Wu, Q.; Zhang, Z.; Shao, Z. Reconstruction with 3D-printed prostheses after sacroiliac joint tumor resection: a retrospective case-control study. *Front Oncol.* **2021**, *11*, 764938.

7. Wang, B.; Hao, Y.; Pu, F.; Jiang, W.; Shao, Z. Computer-aided designed, three dimensional-printed hemipelvic prosthesis for peri-acetabular malignant bone tumour. *Int Orthop.* **2018**, *42*, 687-694.

8. Liu, W.; Shao, Z.; Rai, S.; Hu, B.; Wu, Q.; Hu, H.; Zhang, S.; Wang, B. Three-dimensional-printed intercalary prosthesis for the reconstruction of large bone defect after joint-preserving tumor resection. *J Surg Oncol.* **2020**, *121*, 570-577.

9. Hu, H.; Liu, W.; Zeng, Q.; Wang, S.; Zhang, Z.; Liu, J.; Zhang, Y.; Shao, Z.; Wang, B. The personalized shoulder reconstruction assisted by 3D printing technology after resection of the proximal humerus tumours. *Cancer Manag Res.* **2019**, *11*, 10665-10673.

10. Wu, J.; Xie, K.; Luo, D.; Wang, L.; Wu, W.; Yan, M.; Ai, S.; Dai, K.; Hao, Y. Three-dimensional printing-based personalized limb salvage and reconstruction treatment of pelvic tumors. *J Surg Oncol.* **2021**, *124*, 420-430.

11. Bolia, I. K.; Savvidou, O. D.; Kang, H. P.; Chatzichristodoulou, N.; Megaloikonomos, P. D.; Mitsiokapa, E.; Mavrogenis, A. F.; Papagelopoulos, P. J. Cross-cultural adaptation and validation of the

Musculoskeletal Tumor Society (MSTS) scoring system and Toronto Extremity Salvage Score (TESS) for musculoskeletal sarcoma patients in Greece. *Eur J Orthop Surg Traumatol.* **2021**, *31*, 1631-1638.

12. Chen, X.; Xu, L.; Wang, Y.; Hao, Y.; Wang, L. Image-guided installation of 3D-printed patient-specific implant and its application in pelvic tumor resection and reconstruction surgery. *Comput Methods Programs Biomed.* **2016**, *125*, 66-78.

13. Hao, Y.; Luo, D.; Wu, J.; Wang, L.; Xie, K.; Yan, M.; Dai, K.; Hao, Y. A novel revision system for complex pelvic defects utilizing 3D-printed custom prosthesis. *J Orthop Translat.* **2021**, *31*, 102-109.

14. Li, X.; Ji, T.; Huang, S.; Wang, C.; Zheng, Y.; Guo, W. Biomechanics study of a 3D printed sacroiliac joint fixed modular hemipelvic endoprosthesis. *Clin Biomech (Bristol, Avon).* **2020**, *74*, 87-95.

15. Ji, T.; Yang, Y.; Tang, X.; Liang, H.; Yan, T.; Yang, R.; Guo, W. 3D-printed modular hemipelvic endoprosthetic reconstruction following periacetabular tumor resection: early results of 80 consecutive cases. *J Bone Joint Surg Am.* **2020**, *102*, 1530-1541.

16. Wei, R.; Guo, W.; Ji, T.; Zhang, Y.; Liang, H. One-step reconstruction with a 3D-printed, custom-made prosthesis after total en bloc sacrectomy: a technical note. *Eur Spine J.* **2017**, *26*, 1902-1909.

17. Cai, H.; Liu, Z.; Wei, F.; Yu, M.; Xu, N.; Li, Z. 3D printing in spine surgery. *Adv Exp Med Biol.* **2018**, *1093*, 345-359.

18. Xie, K.; Guo, Y.; Zhao, S.; Wang, L.; Wu, J.; Tan, J.; Yang, Y.; Wu, W.; Jiang, W.; Hao, Y. Partially melted Ti6Al4V particles increase bacterial adhesion and inhibit osteogenic activity on 3D-printed implants: an in vitro study. *Clin Orthop Relat Res.* **2019**, *477*, 2772-2782.

19. Jing, Z.; Zhang, T.; Xiu, P.; Cai, H.; Wei, Q.; Fan, D.; Lin, X.; Song, C.; Liu, Z. Functionalization of 3D-printed titanium alloy orthopedic implants: a literature review. *Biomed Mater.* **2020**, *15*, 052003.

20. Hua, L.; Lei, T.; Qian, H.; Zhang, Y.; Hu, Y.; Lei, P. 3D-printed porous tantalum: recent application in various drug delivery systems to repair hard tissue defects. *Expert Opin Drug Deliv.* **2021**, *18*, 625-634.

21. Wang, H.; Su, K.; Su, L.; Liang, P.; Ji, P.; Wang, C. Comparison of 3D-printed porous tantalum and titanium scaffolds on osteointegration and osteogenesis. *Mater Sci Eng C Mater Biol Appl.* **2019**, *104*, 109908.

22. Wei, X.; Liu, B.; Liu, G.; Yang, F.; Cao, F.; Dou, X.; Yu, W.; Wang, B.; Zheng, G.; Cheng, L.; Ma, Z.; Zhang, Y.; Yang, J.; Wang, Z.; Li, J.; Cui, D.; Wang, W.; Xie, H.; Li, L.; Zhang, F.; Lineaweaver, W. C.; Zhao, D. Mesenchymal stem cell-loaded porous tantalum integrated with biomimetic 3D collagen-based scaffold to repair large osteochondral defects in goats. *Stem Cell Res Ther.* **2019**, *10*, 72.

23. Zhang, T.; Wei, Q.; Fan, D.; Liu, X.; Li, W.; Song, C.; Tian, Y.; Cai, H.; Zheng, Y.; Liu, Z. Improved osseointegration with rhBMP-2 intraoperatively loaded in a specifically designed 3D-printed porous Ti6Al4V vertebral implant. *Biomater Sci.* **2020**, *8*, 1279-1289.

24. Yin, C.; Zhang, T.; Wei, Q.; Cai, H.; Cheng, Y.; Tian, Y.; Leng, H.; Wang, C.; Feng, S.; Liu, Z. Surface treatment of 3D printed porous Ti6Al4V implants by ultraviolet photofunctionalization for improved osseointegration. *Bioact Mater.* **2022**, *7*, 26-38.

25. Zhang, T.; Wei, Q.; Zhou, H.; Zhou, W.; Fan, D.; Lin, X.; Jing, Z.; Cai, H.; Cheng, Y.; Liu, X.; Li, W.; Song, C.; Tian, Y.; Xu, N.; Zheng, Y.; Liu, Z. Sustainable release of vancomycin from micro-arc oxidised 3D-printed porous Ti6Al4V for treating methicillin-resistant Staphylococcus aureus bone infection and enhancing osteogenesis in a rabbit tibia osteomyelitis model. *Biomater Sci.* **2020**, *8*, 3106-3115.

26. Xu, L.; Qin, H.; Cheng, Z.; Jiang, W. B.; Tan, J.; Luo, X.; Huang, W. 3D-printed personalised prostheses for bone defect repair and reconstruction following resection of metacarpal giant cell tumours. *Ann Transl Med.* **2021**, *9*, 1421.

27. Xu, L.; Qin, H.; Tan, J.; Cheng, Z.; Luo, X.; Tan, H.; Huang, W. Clinical study of 3D printed personalized prosthesis in the treatment of bone defect after pelvic tumor resection. *J Orthop Translat.* **2021**, *29*, 163-169.

28. Beltrami, G.; Ristori, G.; Nucci, A. M.; Galeotti, A.; Tamburini, A.; Scoccianti, G.; Campanacci, D.; Innocenti, M.; Capanna, R. Custom-made 3D-printed implants as novel approach to reconstructive surgery after oncologic resection in pediatric patients. *J Clin Med.* **2021**, *10*, 1056.